

Viscoelastic or Viscoplastic Glucose Theory (VGT #58): Using the VGT Energy and Frequency Energy to Estimate the Relative Energy Associated with Diabetic Retinopathy (DR) Risk Probability Percentages under the Influence of Lab-Tested A1C (L.A1C) and Finger-Pierced A1C (F.A1C) over Two 6-Year Periods, Y2010-Y2015 Versus Y2016-Y2021 Based on GH-Method: Math-Physical Medicine (No. 646)

Gerald C Hsu

EclaireMD Foundation, USA

***Corresponding author**

Gerald C Hsu, EclaireMD Foundation, USA

Submitted: 15 Jun 2022; **Accepted:** 21 Jun 2022; **Published:** 09 Jul 2022

Citation: Gerald C Hsu .(2022). *Viscoelastic or Viscoplastic Glucose Theory (VGT #58): Using the VGT Energy and Frequency Energy to Estimate the Relative Energy Associated with Diabetic Retinopathy (DR) Risk Probability Percentages under the Influence of Lab-Tested A1C (L.A1C) and Finger-Pierced A1C (F.A1C) over Two 6-Year Periods, Y2010-Y2015 Versus Y2016-Y2021 Based on GH-Method: Math-Physical Medicine (No. 646).* *J App Mat Sci & Engg Res*, 6(2), 01-12.

Abstract

The author was a professional engineer working in the fields of space shuttle, naval battleships, nuclear power plants, computer hardware and software, artificial intelligence, and semiconductor chips. After his retirement, he started to self-study and research internal medicine, emphasizing biomarker relationships exploration and disease prevention. Since 2010, he has utilized the disciplines learned from 7 different universities along with various work experiences to formulate his current medical research work during the past 13 years.

In engineering and medicine, he discovered that we frequently seek answers, illustrations, or explanations for the relationships between the input variable (force applied on a structure or cause of a disease) and output variable (deformation of a structure or symptom of a disease). However, the multiple relationships between input and output could be expressed with many different matrix formats of 1×1 , $1 \times n$, $m \times 1$, or $m \times n$ (m or n means different multiple variables). In addition to these described mathematical complications, the output resulting from one or more inputs can also become an input of another output, which is a symptom of certain causes that can become a cause of another different symptom. This phenomenon is a complex scenario with "chain effects". In fact, engineering and biomedical complications are fundamentally mathematical problems that correlate or conform with many inherent physical laws or principles.

Over the past 13 years, in his medical research, he has encountered more than 100 different sets of biomarkers with almost equal amounts of cause/input variables versus symptom/output variables. For example, food and exercise influence both body weight and glucose level, where persistent high glucose can result in diabetes.

When diabetes combines with hypertension (high blood pressure) and hyperlipidemia (high blood lipids), it can cause diabetic retinopathy (DR), cardiovascular disease (CVD), or chronic kidney disease (CKD). Furthermore, obesity and diabetes are also linked with various kinds of cancers.

Diabetic retinopathy (DR) occurs when too much blood sugar or glucose damages the blood vessels in the retina. As a result, the retina does not get enough oxygen and nutrients, and blood vessels can leak blood into the retina. DR is the leading cause of new cases of blindness in people 20 to 74 years of age in the US (Reference: Eylea, Regeneron Pharmaceuticals, Inc.).

The author has researched these multiple sets of biomedical input versus output using different tools he has learned from academic fields of mathematics, physics, computer science, and engineering. For example, he has applied a signal processing technique to separate 19 components from the combined postprandial plasma glucose (PPG) wave. He identified the carbs/sugar intake amount and post-meal exercise as the two most important contributing factors to PPG formation. Based on these findings, he then applied the theory of elasticity to develop a linear elastic glucose

theory (LEGT) to predict PPG value with high prediction accuracy, using fasting plasma glucose (FPG), carbs/sugar intake grams, and post-meal walking k-steps as three major input components of predicted PPG formation.

Furthermore, he took a specific PPG waveform in the time domain (TD) and applied the fast Fourier transform (FFT) technique to convert it into a waveform in the frequency domain (FD). The y-axis value in the frequency diagram indicates the magnitude of energy corresponding to a certain frequency component on the x-axis, while the total area underneath the frequency-energy curve is the total relative energy associated with this specific PPG wave. He calls this relative energy the “frequency energy”.

Recently, he also applied the theories of viscoelasticity and viscoplasticity (VGT) in physics and engineering to various biomedical problems and has written more than 50 biomedical research papers. This VGT application emphasizes the time-dependency characteristics of certain variables. In the medical field, most biomarkers are time-dependent since body organ cells are organic in nature and change all of the time. Incidentally, VGT can generate a stress-strain curve or cause-symptom curve (known as a “hysteresis loop” in physics), in which area size can also be used to estimate the relative energy created during the process of uploading (digesting carbs/sugar) and unloading (walking exercise) over the timespan of a biomarker’s wave, such as PPG or CKD risk %. He calls this relative energy “VGT energy”.

Body weight (BW) is easily measured by using a bathroom scale. Weight in the early morning is highly correlated (his data shows ~90% of the correlation coefficient) with fasting plasma glucose (FPG) measured in the early morning or average glucose during sleeping hours. FPG also serves as the baseline of postprandial plasma glucose (PPG) and contributes around 25% to 29% of daily estimated average glucose (eAG). Daily average glucose levels or quarterly HbA1C values (average eAG over the past 90-115 days divided by a conversion factor) determine the severity of diabetes. This medical condition is one of the major influential chronic diseases that may increase certain risk factors for heart diseases, such as CVD (mainly artery blockage or rupture problems) or CKD (mainly micro-vessels leakage issues). Diabetes is also related to many types of cancers based on the common root causes, regardless of vast differences in symptoms.

From 2010 to 2011, the author collected sparse biomarker data, but beginning in 2012, he has been gathering BW and finger-piercing glucose values each day. In addition, he accumulates medical conditions data including blood pressure (BP), heart rate (HR), and blood lipids along with lifestyle details (LD). Based on the collected big data, he further organized them into two main groups. The first is the medical conditions group (MC) with 4 categories: weight, glucose, BP, and blood lipids. The second is the LD group with 6 categories: food & diet, exercise, water intake, sleep, stress, and daily routines. At first, he collected his data daily since Y2012 and then calculated a unique combined daily score for each of the 10 categories within the MC and LD groups. The combined scores of the 2 groups, 10 categories, and 500+ detailed elements constitute an overall “metabolism index (MI) model”. This model was developed in Y2014 by the author using the topology concept, nonlinear algebra, geometric algebra, and engineering finite element method. It includes the root causes of 6 major lifestyle inputs and symptoms from 4 rudimentary chronic diseases: obesity, diabetes, hypertension, and hyperlipidemia. Therefore, the MI model, especially its 4 chronic disease conditions, can be used as the foundation and building block for his additional research work that can expand into various complications associated with different organs, such as DR, CVD, CKD, and various cancers.

Within the MI model, the rudimentary chronic diseases from the 6 LD influence more complicated diseases, such as heart problems (CVD & CHD), CKD, stroke, DR, neuropathy, hypothyroidism, diabetic constipation, diabetic skin fungal infection, and many others including cancers and dementia. Some genetic conditions and lifetime unhealthy habits, which include smoking, alcohol consumption, and illicit drug use, account for approximately 15% to 25% of the root cause of chronic diseases along with their complications, as well as cancers and dementia. Some external factors, environmental influences, and viral infections, such as radiation, air and water pollution, food poison and pollution, toxic chemicals, and hormonal therapy can also contribute to the causes of cancers.

All of the above-mentioned diseases fall into the category of “symptoms” which are the outcomes of “root causes” of poor living environments and unhealthy lifestyles.

His calculated risk probability % for CKD, CVD, stroke and various cancers have differences in their root-cause variables, their associated weighting factors, and certain biomedical assumptions. Specifically, the CVD/Stroke risk includes two major scenarios that combine emphasized weighting factors, blood vessel blockage due to blood glucose and blood lipids, and blood vessel rupture caused by blood glucose and BP. **There is evidence of a relationship between BP and DR (Reference: BP control and DR, by R. Klein and BEK Klein from British Journal of Ophthalmology).** The CKD risks include hyperglycemic damage to micro-blood vessels and nerves which causes protein leakage found in urine and waste deposit within the kidneys; therefore, it requires dialysis to remove waste products and excess fluids from the body. However, the cancer risk consists of additional influential factors from environmental conditions and viral infections, on top of genetic conditions (DNA and family history), 3-lifetime unhealthy habits (drinking, smoking, and illicit drugs), 4 chronic medical conditions, along with 6 LD which is identical in the DR, CVD, and CKD risk categories.

Since December 2021, the author applied theories of viscoelasticity and viscoplasticity (VGT) from physics and en-

gineering disciplines to investigate more than 50 sets of input/output biomarkers. The purpose is to identify certain hidden relationships between certain output biomarkers, DR risk, CKD risk, CVD risk, or Cancer risk, along with their corresponding input biomarkers, such as HbA1C, ACR, eAG, BW, and FPG measured either during sleeping hours or in the early morning.

In this study, the hidden biophysical behaviors and possible inter-relationships among the three biomarkers, DR risk % vs. lab A1C and finger A1C, are “time-dependent” and change from time to time. **This important time-dependency characteristic provides insight into the DR risk’s moving pattern. It covers curve shape, the associated energy created or stored inside during the process of stress up-loading (moving upward or increasing) and stress down-loading (moving downward or decreasing) of the input biomarkers of lab A1C or finger A1C along with the output biomarker of DR risk %.**

The objective of this research article is to explore a possible link between DR risk probability percentage (DR risk %) versus lab A1C and finger A1C, using the VGT energy model and the frequency energy model. In this article, he selects 12 years of collected data and then groups them into two 6-year periods, Y2010-Y2015 and Y2016-Y2021. Within each period, he uses 6 individual annual data. These datasets contain 3 key biomarkers, DR risk % as the symptom (output) along with lab A1C and finger A1C as the causes (inputs) to conduct his VGT analysis. Now, he can apply VGT specifically to construct 2 stress-strain diagrams with 2 hysteresis loop areas that correspond to the energy status from the input variable of lab A1C and finger A1C. The purpose of this study is to obtain and compare the calculated relative energy levels in each period using the VGT energy approach. In addition, he converts the two DR risk % waveforms in a time domain into a frequency domain. He then calculates the total area underneath the two frequency waveforms as his frequency energies to compare against the VGT energies.

The following defined stress and strain equations are used to establish the VGT stress-strain diagram in a space domain (SD):

VGT strain

= ε (symptom)

= individual symptom at the present time

VGT Stress

= σ (based on the change rate of strain, symptom, multiplying with one or more viscosity factors or causes)

= $\eta * (d\varepsilon/dt)$

= $\eta * (d\text{-strain}/d\text{-time})$

= (viscosity factor η using normalized cause at present time) * (symptom at present time - symptom at a previous time)

Where the strain is DR risk % and the stress is DR risk change rate multiplied by his lab A1C or finger A1C as two viscosity factors. In this study, he uses 6.0 as his two normalization factors for the lab A1C and finger A1C, respectively. 6.0% is the dividing line between diabetes-free and pre-diabetes.

To offer a simple explanation to readers who do not have a physics or engineering background, the author includes a brief excerpt from Wikipedia regarding the description of basic concepts for elasticity and plasticity theories, viscoelasticity, and viscoplasticity theories from the disciplines of engineering and physics in the Method section.

In conclusion, the following five described biophysical characteristics have demonstrated the key behaviors of DR risk % using the approaches of both VGT energy and the frequency energy:

(1) When his body weight drops continuously over these two 6-year periods, both the lab A1C and finger A1C values also decrease. His lab ACR and finger A1C have a **strong correlation coefficient (R = 86%)**. This reduction of lab A1C and finger A1C can be seen clearly from the attached data table. **His 6-year average data of (lab A1C, finger A1C) are: Y10-15 = (7.3%, 8.5%) and Y16-21 = (6.5%, 6.7%). His 6-year average DR risks are: Y10-15 = 74% and Y16-21 = 54%.**

(2) **Looking into the 2 average strain (DR risk %) values for the two periods, the Y10-15 period covers a DR risk range of 60%-100% with an average DR risk of 74%, while the Y16-21 period includes a DR risk range of 52%-56% with an average DR risk of 54%.**

(3) His annual lab A1C and finger A1C values within the two 6-year periods are continuously declining as time moves forward. This observed phenomenon provides a clue that the viscosity factors, η = lab A1C and finger A1C, are also decreasing as time moves forward. Therefore, the stress magnitudes based on lab A1C and finger A1C are reduced from the first 6-year period to the second 6-year period since stress is the strain rate multiplied by the viscosity factor of η . See the lab A1C stress-range, or lab A1C y-axis scale: **Y10-15 = 19 (0 to -18.8) and Y16-21 = 5 (2.2 to -2.6)**. The finger A1C stress range or finger A1C y-axis scale is: **Y10-15 = 26 (0.5 to -25.5) and Y16-21 = 5 (2.3 to -2.5)**. One observation is that the Y10-15 lab A1C stress ranges (-7.5) are fairly close to the Y10-15 finger ACR stress ranges (-9.1); while the Y16-21 lab A1C stress ranges (-0.8) are identical to the Y16-21 finger ACR stress-ranges (-0.8).

It should be mentioned that **the normalized factor for both lab A1C and finger A1C is 6.0%.**

(4) The calculated 2 hysteresis loop areas are **significantly reduced from the first 6-year period to the second 6-year period, the lab A1C area reduction rate is 67 while the finger A1C area reduction rate is 85.** These two-loop areas represent the associated relative energy of DR risk under the influence of lab A1C and finger A1C within each period. See the lab A1C hysteresis loop areas: Y10-15 = 427 and Y16-21 = 6 and the finger A1C hysteresis loop areas: Y10-15 = 540 and Y16-21 = 6. Based on the above 4 loop areas, it is obvious that **the VGT energies for the Y10-15 period are about 67 to 85 times higher than the Y16-21 period.**

(5) Using the frequency energy tool, the comparison between Y10-15 period versus Y16-21 are: average DR risk % in TD = 74% vs. 55% with a ratio of DR risk $5 = 74/55 = 1.35$, while the DR risk frequency energy in a FD = 1376 vs. 14 with a ratio of DR frequency energy = $1376/14 = 99.7$. **This significant frequency energy difference of 99.7 is similar to the VGT energy difference of 67-85.**

In summary, body weight influences glucose. The energy in glucose circulates with the blood flow inside the body. If we have excessive energy associated with hyperglycemia within the blood flow, it can damage internal organs to cause retinal complications, including DR.

From this study of biomarker data analysis within a long 12-year period which is grouped into two identical 6-year sub-periods, **the energy ratios for the two periods (Y10-15 versus Y16-21) are re-listed in a simplified fashion:**

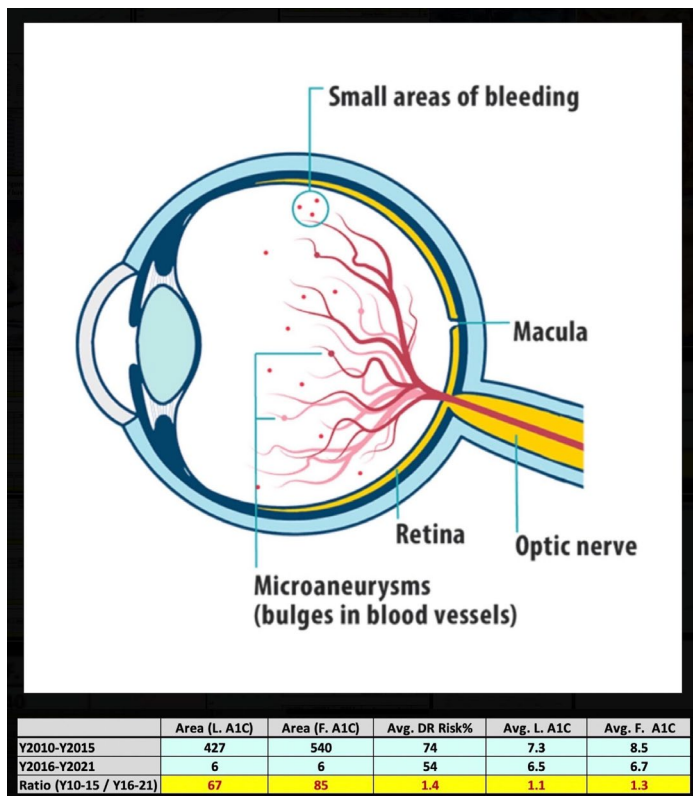
(1) Energy ratio of Y10-15 versus Y16-21 using VGT method: lab A1C loop area ratio = 67 to 1; finger A1C loop area ratio = 85 to 1.

(2) Metabolism index-based CKD risk ratio of Y10-15 versus Y16-21 = 1.4 to 1.

(3) Collected average lab A1C ratio of Y10-15 versus Y16-21 = 1.1 to 1.

(4) collected average finger A1C ratio of Y10-15 versus Y16-21 = 1.3 to 1.

The two energy ratios of DR risk (both A1C-based and ACR-based) have similar patterns. When BW and daily glucose conditions improve, his DR risks are then reduced accordingly (by 40%); however, the associated energies with DR risks are decreased even more significantly (by 67-85 times if using the VGT energy method or 99.7 times if using the frequency energy method). **It should be pointed out that his DR risk was remarkably reduced in the second 6-year period when his lab A1C and finger A1C dropped below 6.7%, since the dividing year between healthy versus unhealthy in Y2016.**



Introduction

The author was a professional engineer working in the fields of the space shuttle, naval battleships, nuclear power plants, com-

puter hardware and software, artificial intelligence, and semiconductor chips. After his retirement, he started to self-study and research internal medicine, emphasizing biomarker relationships exploration and disease prevention. Since 2010, he has utilized the disciplines learned from 7 different universities along with various work experiences to formulate his current medical research work during the past 13 years.

In engineering and medicine, he discovered that we frequently seek answers, illustrations, or explanations for the relationships between the input variable (force applied on a structure or cause of a disease) and output variable (deformation of a structure or symptom of a disease). However, the multiple relationships between input and output could be expressed with many different matrix formats of 1×1 , $1 \times n$, $m \times 1$, or $m \times n$ (m or n means different multiple variables). In addition to these described mathematical complications, the output resulting from one or more inputs can also become an input of another output, which is a symptom of certain causes that can become a cause of another different symptom. This phenomenon is a complex scenario with "chain effects". In fact, engineering and biomedical complications are fundamentally mathematical problems that correlate or conform with many inherent physical laws or principles.

Over the past 13 years, in his medical research, he has encountered more than 100 different sets of biomarkers with almost equal amounts of cause/input variables versus symptom/output variables. For example, food and exercise influence both body

weight and glucose level, where persistent high glucose can result in diabetes.

When diabetes combines with hypertension (high blood pressure) and hyperlipidemia (high blood lipids), it can cause diabetic retinopathy (DR), cardiovascular disease (CVD), or chronic kidney disease (CKD). Furthermore, obesity and diabetes are also linked with various kinds of cancers.

Diabetic retinopathy (DR) occurs when too much blood sugar or glucose damages the blood vessels in the retina. As a result, the retina does not get enough oxygen and nutrients, and blood vessels can leak blood into the retina. DR is the leading cause of new cases of blindness in people 20 to 74 years of age in the US (*Reference: Eylea, Regeneron Pharmaceuticals, Inc.*).

The author has researched these multiple sets of biomedical input versus output using different tools he has learned from academic fields of mathematics, physics, computer science, and engineering. For example, he has applied a signal processing technique to separate 19 components from the combined postprandial plasma glucose (PPG) wave. He identified the carbs/sugar intake amount and post-meal exercise as the two most important contributing factors to PPG formation. Based on these findings, he then applied the theory of elasticity to develop a linear elastic glucose theory (LEGT) to predict PPG value with high prediction accuracy, using fasting plasma glucose (FPG), carbs/sugar intake grams, and post-meal walking k-steps as three major input components of predicted PPG formation.

Furthermore, he took a specific PPG waveform in the time domain (TD) and applied the fast Fourier transform (FFT) technique to convert it into a waveform in the frequency domain (FD). The y-axis value in the frequency diagram indicates the magnitude of energy corresponding to a certain frequency component on the x-axis, while the total area underneath the frequency-energy curve is the total relative energy associated with this specific PPG wave. *He calls this relative energy the "frequency energy"*.

Recently, he also applied the theories of viscoelasticity and viscoplasticity (VGT) in physics and engineering to various biomedical problems and has written more than 50 biomedical research papers. This VGT application emphasizes the time-dependency characteristics of certain variables. In the medical field, most biomarkers are time-dependent since body organ cells are organic in nature and change all of the time. Incidentally, VGT can generate a stress-strain curve or cause-symptom curve (known as a "*hysteresis loop*" in physics), in which area size can also be used to estimate the relative energy created during the process of uploading (digesting carbs/sugar) and unloading (walking exercise) over the timespan of a biomarker's wave, such as PPG or CKD risk %. He calls this relative energy "*VGT energy*".

Body weight (BW) is easily measured by using a bathroom scale. Weight in the early morning is highly correlated (his data shows ~90% of the correlation coefficient) with fasting plasma glucose (FPG) measured in the early morning or average glucose during sleeping hours. FPG also serves as the baseline of postprandial

plasma glucose (PPG) and contributes around 25% to 29% of daily estimated average glucose (eAG). Daily average glucose levels or quarterly HbA1C values (average eAG over the past 90-115 days divided by a conversion factor) determine the severity of diabetes. This medical condition is one of the major influential chronic diseases that may increase certain risk factors for heart diseases, such as CVD (mainly artery blockage or rupture problems) or CKD (mainly micro-vessels leakage issues). Diabetes is also related to many types of cancers based on the common root causes, regardless of vast differences in symptoms.

From 2010 to 2011, the author collected sparse biomarker data, but beginning in 2012, he has been gathering BW and finger-piercing glucose values each day. In addition, he accumulates medical conditions data including blood pressure (BP), heart rate (HR), and blood lipids along with lifestyle details (LD). Based on the collected big data, he further organized them into two main groups. The first is the medical conditions group (MC) with 4 categories: weight, glucose, BP, and blood lipids. The second is the LD group with 6 categories: food & diet, exercise, water intake, sleep, stress, and daily routines. At first, he collected his data daily since Y2012 and then calculated a unique combined daily score for each of the 10 categories within the MC and LD groups. The combined scores of the 2 groups, 10 categories, and 500+ detailed elements constitute an overall "metabolism index (MI) model". This model was developed in Y2014 by the author using the topology concept, non-linear algebra, geometric algebra, and engineering finite element method. It includes the root causes of 6 major lifestyle inputs and symptoms from 4 rudimentary chronic diseases: obesity, diabetes, hypertension, and hyperlipidemia. Therefore, the MI model, especially its 4 chronic disease conditions, can be used as the foundation and building block for his additional research work that can expand into various complications associated with different organs, such as DR, CVD, CKD, and various cancers.

Within the MI model, the rudimentary chronic diseases from the 6 LD influence more complicated diseases, such as heart problems (CVD & CHD), CKD, stroke, DR, neuropathy, hypothyroidism, diabetic constipation, diabetic skin fungal infection, and many others including cancers and dementia. Some genetic conditions and lifetime unhealthy habits, which include smoking, alcohol consumption, and illicit drug use, account for approximately 15% to 25% of the root cause of chronic diseases along with their complications, as well as cancers and dementia. Some external factors, environmental influences, and viral infections, such as radiation, air and water pollution, food poison and pollution, toxic chemicals, and hormonal therapy can also contribute to the causes of cancers.

All of the above-mentioned diseases fall into the category of "symptoms" which are the outcomes of "root causes" of poor living environments and unhealthy lifestyles.

His calculated risk probability % for CKD, CVD, stroke, and various cancers have differences in their root-cause variables, their associated weighting factors, and certain biomedical assumptions. *Specifically, the CVD/Stroke risk includes two major scenarios that combine emphasized weighting factors, blood*

vessel blockage due to blood glucose and blood lipids, and blood vessel rupture caused by blood glucose and BP. **There is evidence of a relationship between BP and DR (Reference: BP control and DR, by R. Klein and BEK Klein from British Journal of Ophthalmology).** The CKD risks include hyperglycemic damage to micro-blood vessels and nerves which causes protein leakage found in urine and waste deposit within the kidneys; therefore, it requires dialysis to remove waste products and excess fluids from the body. However, the cancer risk consists of additional influential factors from environmental conditions and viral infections, on top of genetic conditions (DNA and family history), 3-lifetime unhealthy habits (drinking, smoking, and illicit drugs), 4 chronic medical conditions, along with 6 LD which are identical in the DR, CVD, and CKD risk categories.

Since December 2021, the author applied theories of viscoelasticity and viscoplasticity (VGT) from physics and engineering disciplines to investigate more than 50 sets of input/output biomarkers. The purpose is to identify certain hidden relationships between certain output biomarkers, DR risk, CKD risk, CVD risk, or Cancer risk, along with their corresponding input biomarkers, such as HbA1C, ACR, eAG, BW, and FPG measured either during sleeping hours or in the early morning.

In this study, the hidden biophysical behaviors and possible inter-relationships among the three biomarkers, DR risk % vs. lab A1C and finger A1C, are “time-dependent” and change from time to time. This important time-dependency characteristic provides insight into the DR risk’s moving pattern. It covers curve shape, the associated energy created or stored inside during the process of stress up-loading (moving upward or increasing) and stress down-loading (moving downward or decreasing) of the input biomarkers of lab A1C or finger A1C along with the output biomarker of DR risk %.

The objective of this research article is to explore a possible link between DR risk probability percentage (DR risk %) versus lab A1C and finger A1C, using the VGT energy model and the frequency energy model. In this article, he selects 12 years of collected data and then groups them into two 6-year periods, Y2010-Y2015 and Y2016-Y2021. Within each period, he uses 6 individual annual data. These datasets contain 3 key biomarkers, DR risk% as the symptom (output) along with lab A1C and finger A1C as the causes (inputs) to conduct his VGT analysis. Now, he can apply VGT specifically to construct 2 stress-strain diagrams with 2 hysteresis loop areas that correspond to the energy status from the input variable of lab A1C and finger A1C. The purpose of this study is to obtain and compare the calculated relative energy levels in each period using the VGT energy approach. In addition, he converts the two DR risk % waveforms in a time domain into a frequency domain. He then calculates the total area underneath the two frequency waveforms as his frequency energies to compare against the VGT energies.

The following defined stress and strain equations are used to establish the VGT stress-strain diagram in a space domain (SD):

VGT strain
= ε (symptom)

= individual symptom at the present time

VGT Stress

= σ (based on the change rate of strain, symptom, multiplying with one or more viscosity factors or causes)

= $\eta * (d\varepsilon/dt)$

= $\eta * (d\text{-strain}/d\text{-time})$

= (viscosity factor η using normalized cause at present time) * (symptom at present time - symptom at a previous time)

Where the strain is DR risk % and the stress is DR risk change rate multiplied by his lab A1C or finger A1C as two viscosity factors.

In this study, he uses 6.0 as his two normalization factors for the lab A1C and finger A1C, respectively. 6.0% is the dividing line between diabetes-free and pre-diabetes.

To offer a simple explanation to readers who do not have a physics or engineering background, the author includes a brief excerpt from Wikipedia regarding the description of basic concepts for elasticity and plasticity theories, viscoelasticity, and viscoplasticity theories from the disciplines of engineering and physics in the Method section.

Methods

Elasticity, Plasticity, Viscoelasticity, and Viscoplasticity

The Difference Between Elastic Materials and Viscoelastic Materials

(from “Soborthans, innovating shock and vibration solutions”)

What are elastic materials?

Elasticity is the tendency of solid materials to return to their original shape after forces are applied to them. When the forces are removed, the object will return to its initial shape and size if the material is elastic.

What are viscous materials?

Viscosity is a measure of a fluid’s resistance to flow. A fluid with large viscosity resists motion. A fluid with low viscosity flows. For example, water flows more easily than syrup because it has a lower viscosity. High viscosity materials might include honey, syrups, or gels – generally things that resist flow. Water is a low viscosity material, as it flows readily. Viscous materials are thick or sticky or adhesive. Since heating reduces viscosity, these materials don’t flow easily. For example, warm syrup flows more easily than cold.

What is viscoelastic?

Viscoelasticity is the property of materials that exhibit both viscous and elastic characteristics when undergoing deformation. Synthetic polymers, wood, and human tissue, as well as metals at high temperature, display significant viscoelastic effects. In some applications, even a small viscoelastic response can be significant.

Elastic behavior versus viscoelastic behavior

The difference between elastic materials and viscoelastic ma-

materials is that viscoelastic materials have a viscosity factor and the elastic ones don't. Because viscoelastic materials have the viscosity factor, they have a strain rate dependent on time. Purely elastic materials do not dissipate energy (heat) when a load is applied, then removed; however, a viscoelastic substance does.

The following brief introductions are excerpts from Wikipedia:

“Elasticity (physics)

The physical property is when materials or objects return to their original shape after deformation

In physics and materials science, **elasticity** is the ability of a body to resist a distorting influence and to return to its original size and shape when that influence or force is removed. Solid objects will deform when adequate loads are applied to them; if the material is elastic, the object will return to its initial shape and size after removal. This is in contrast to plasticity, in which the object fails to do so and instead remains in its deformed state.

The physical reasons for elastic behavior can be quite different for different materials. In metals, the atomic lattice changes size and shape when forces are applied (energy is added to the system). When forces are removed, the lattice goes back to the original lower energy state. For rubbers and other polymers, elasticity is caused by the stretching of polymer chains when forces are applied.

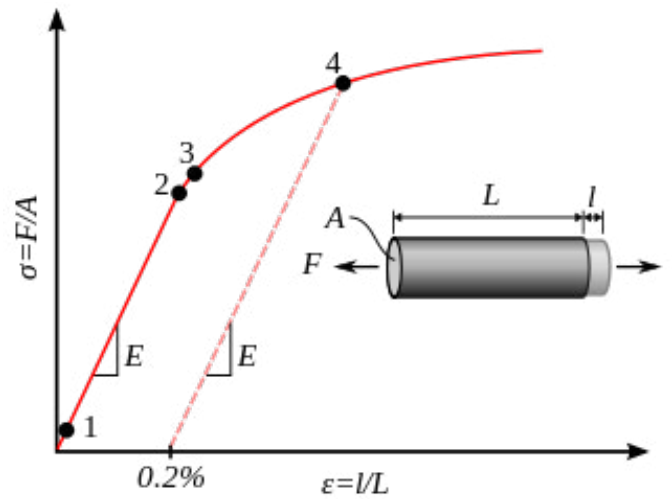
Hooke's law states that the force required to deform elastic objects should be directly proportional to the distance of deformation, regardless of how large that distance becomes. This is known as perfect elasticity, in which a given object will return to its original shape no matter how strongly it is deformed. This is an ideal concept only; most materials that possess elasticity in practice remain purely elastic only up to very small deformations, after which plastic (permanent) deformation occurs.

In engineering, the elasticity of a material is quantified by the elastic modulus such as Young's modulus, bulk modulus, or shear modulus which measure the amount of stress needed to achieve a unit of strain; a higher modulus indicates that the material is harder to deform. The material's elastic limit or yield strength is the maximum stress that can arise before the onset of plastic deformation.

Plasticity (physics)

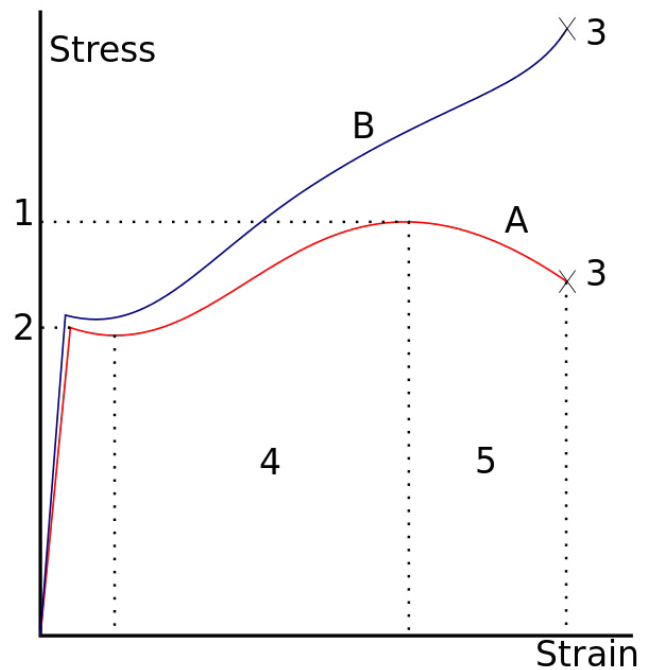
Deformation of a solid material undergoing non-reversible changes of shape in response to applied forces.

In physics and materials science, **plasticity**, also known as **plastic deformation**, is the ability of a solid material to undergo permanent deformation, a non-reversible change of shape in response to applied forces. For example, a solid piece of metal being bent or pounded into a new shape displays plasticity as permanent changes occur within the material itself. In engineering, the transition from elastic behavior to plastic behavior is known as yielding.



A stress-strain curve showing typical yield behavior for nonferrous alloys.

1. True elastic limit
2. Proportionality limit
3. Elastic limit
4. Offset yield strength



A stress-strain curve is typical of structural steel.

- 1: Ultimate strength
- 2: Yield strength (yield point)
- 3: Rupture
- 4: Strain hardening region
- 5: Necking region
- A: Apparent stress (F/A_0)
- B: Actual stress (F/A)

Plastic deformation is observed in most materials, particularly metals, soils, rocks, concrete, and foams. However, the physical mechanisms that cause plastic deformation can vary widely. At a crystalline scale, plasticity in metals is usually a consequence

of dislocations. Such defects are relatively rare in most crystalline materials, but are numerous in some and part of their crystal structure; in such cases, plastic crystallinity can result. In brittle materials such as rock, concrete, and bone, plasticity is caused predominantly by slip at microcracks. In cellular materials such as liquid foams or biological tissues, plasticity is mainly a consequence of bubble or cell rearrangements, notably TI processes.

For many ductile metals, tensile loading applied to a sample will cause it to behave in an elastic manner. Each increment of load is accompanied by a proportional increment in extension. When the load is removed, the piece returns to its original size. However, once the load exceeds a threshold – the yield strength – the extension increases more rapidly than in the elastic region; now when the load is removed, some degree of extension will remain. Elastic deformation, however, is an approximation and its quality depends on the time frame considered and loading speed. If, as indicated in the graph opposite, the deformation includes elastic deformation, it is also often referred to as "elasto-plastic deformation" or "elastic-plastic deformation".

Perfect plasticity is a property of materials to undergo irreversible deformation without any increase in stresses or loads. Plastic materials that have been hardened by prior deformation, such as cold forming, may need increasingly higher stresses to deform further. Generally, plastic deformation is also dependent on the deformation speed, i.e. higher stresses usually have to be applied to increase the rate of deformation. Such materials are said to deform visco-plastically."

Viscoelasticity

Property of materials with both viscous and elastic characteristics under deformation.

In materials science and continuum mechanics, viscoelasticity is the property of materials that exhibit both viscous and elastic characteristics when undergoing deformation. Viscous materials, like water, resist shear flow and strain linearly with time when a stress is applied. Elastic materials strain when stretched and immediately return to their original state once the stress is removed.

Viscoelastic materials have elements of both of these properties and, as such, exhibit time-dependent strain. Whereas elasticity is usually the result of bond stretching along crystallographic planes in an ordered solid, viscosity is the result of the diffusion of atoms or molecules inside an amorphous material.

In the nineteenth century, physicists such as Maxwell, Boltzmann, and Kelvin researched and experimented with creep and recovery of glasses, metals, and rubbers. Viscoelasticity was further examined in the late twentieth century when synthetic polymers were engineered and used in a variety of applications. Viscoelasticity calculations depend heavily on the viscosity variable, η . The inverse of η is also known as fluidity, ϕ . The value of either can be derived as a function of temperature or as a given value (i.e. for a dashpot).

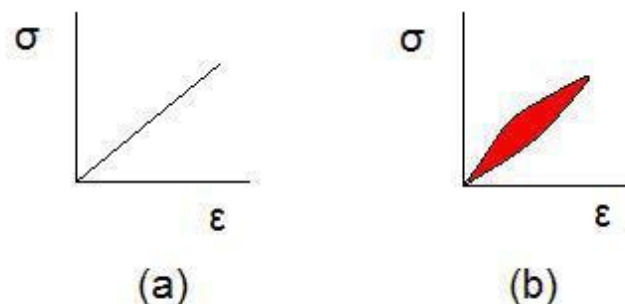
Depending on the change of strain rate versus stress inside a material, the viscosity can be categorized as having a linear, non-linear, or plastic response. When a material exhibits a linear response it is categorized as a Newtonian material. In this case, the stress is linearly proportional to the strain rate. If the material exhibits a non-linear response to the strain rate, it is categorized as Non-Newtonian fluid. There is also an interesting case where the viscosity decreases as the shear/strain rate remains constant. A material that exhibits this type of behavior is known as thixotropic. In addition, when the stress is independent of this strain rate, the material exhibits plastic deformation. Many viscoelastic materials exhibit rubber-like behaviors explained by the thermodynamic theory of polymer elasticity.

Cracking occurs when the strain is applied quickly and outside of the elastic limit. Ligaments and tendons are viscoelastic, so the extent of the potential damage to them depends both on the rate of the change of their length as well as on the force applied.

A viscoelastic material has the following properties:

- hysteresis is seen in the stress-strain curve
- stress relaxation occurs: step constant strain causes decreasing stress
- creep occurs: step constant stress causes increasing strain
- its stiffness depends on the strain rate or the stress rate.

Elastic versus viscoelastic behavior



Stress-strain curves for a purely elastic material (a) and a viscoelastic material (b). The red area is a hysteresis loop and shows the amount of energy lost (as heat) in a loading and unloading cycle. It is equal to

$\oint \sigma d\epsilon$

where σ is stress and ϵ is strain.

Unlike purely elastic substances, a viscoelastic substance has an elastic component and a viscous component. **The viscosity of a viscoelastic substance gives the substance a strain rate dependence on time.** Purely elastic materials do not dissipate energy (heat) when a load is applied, then removed. However, a viscoelastic substance dissipates energy when a load is **applied, then removed. Hysteresis is observed in the stress-strain curve, with the area of the loop being equal to the energy lost during the loading cycle. Since viscosity is the resistance to thermally activated plastic deformation, a viscous material will lose energy through a loading cycle. Plastic deformation results in lost**

energy, which is uncharacteristic of a purely elastic material's reaction to a loading cycle.

Specifically, viscoelasticity is a molecular rearrangement. When a stress is applied to a viscoelastic material such as a polymer, parts of the long polymer chain change positions. This movement or rearrangement is called “creep”. Polymers remain a solid material even when these parts of their chains are rearranging in order to accompany the stress, and as this occurs, it creates a back stress in the material. When the back stress is the same magnitude as the applied stress, the material no longer creeps. When the original stress is taken away, the accumulated back stresses will cause the polymer to return to its original form. **The material creeps, which gives the prefix visco-, and the material fully recovers, which gives the suffix -elasticity.**

Viscoplasticity

Viscoplasticity is a theory in continuum mechanics that describes the rate-dependent inelastic behavior of solids. Rate-dependence in this context means that the deformation of the material depends on the rate at which loads are applied. The inelastic behavior that is the subject of viscoplasticity is plastic deformation which means that the material undergoes unrecoverable deformations when a load level is reached. Rate-dependent plasticity is important for transient plasticity calculations. The main difference between rate-independent plastic and viscoplastic material models is that the latter exhibit not only permanent deformations after the application of loads but continue to undergo a creep flow as a function of time under the influence of the applied load.

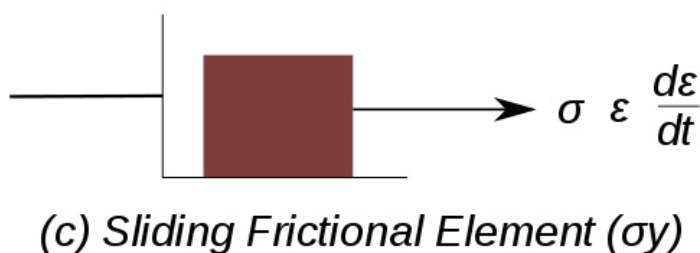
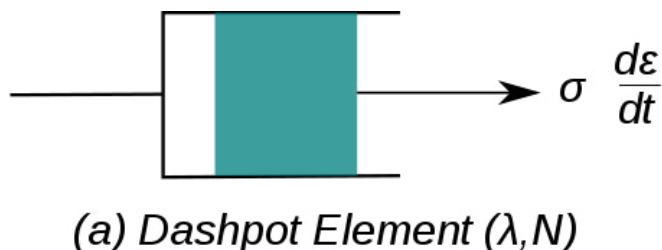


Figure 1: Elements used in one-dimensional models of viscoplastic materials.

The elastic response of viscoplastic materials can be represented in one dimension by Hookean spring elements. Rate-dependence can be represented by nonlinear dashpot elements in a manner similar to viscoelasticity. Plasticity can be accounted for by adding sliding frictional elements as shown in Figure 1. In Figure E is the modulus of elasticity, λ is the viscosity parameter and N is a power-law type parameter that represents non-linear dashpot [$\sigma(d\epsilon/dt) = \sigma = \lambda(d\epsilon/dt)^{1/N}$]. The sliding element can have a yield stress (σ_y) that is strain rate dependent, or even constant, as shown in Figure 1c.

Viscoplasticity is usually modeled in three dimensions using overstress models of the Perzyna or Duvaut-Lions types. In these models, the stress is allowed to increase beyond the rate-independent yield surface upon application of a load and then allowed to relax back to the yield surface over time. The yield surface is usually assumed not to be rate-dependent in such models. An alternative approach is to add a strain rate dependence to the yield stress and use the techniques of rate-independent plasticity to calculate the response of a material. For metals and alloys, viscoplasticity is the macroscopic behavior caused by a mechanism linked to the movement of dislocations in grains, with superposed effects of inter-crystalline gliding. The mechanism usually becomes dominant at temperatures greater than approximately one-third of the absolute melting temperature. However, certain alloys exhibit viscoplasticity at room temperature (300K). For polymers, wood, and bitumen, the theory of viscoplasticity is required to describe behavior beyond the limit of elasticity or viscoelasticity.

In general, viscoplasticity theories are useful in areas such as

- the calculation of permanent deformations,
- the prediction of the plastic collapse of structures,
- the investigation of stability,
- crash simulations,
- systems exposed to high temperatures such as turbines in engines, e.g. a power plant,
- dynamic problems and systems exposed to high strain rates.

Phenomenology

For qualitative analysis, several characteristic tests are performed to describe the phenomenology of viscoplastic materials. Some examples of these tests are

1. hardening tests at constant stress or strain rate,
2. creep tests at constant force, and
3. stress relaxation at constant elongation.

Strain hardening test

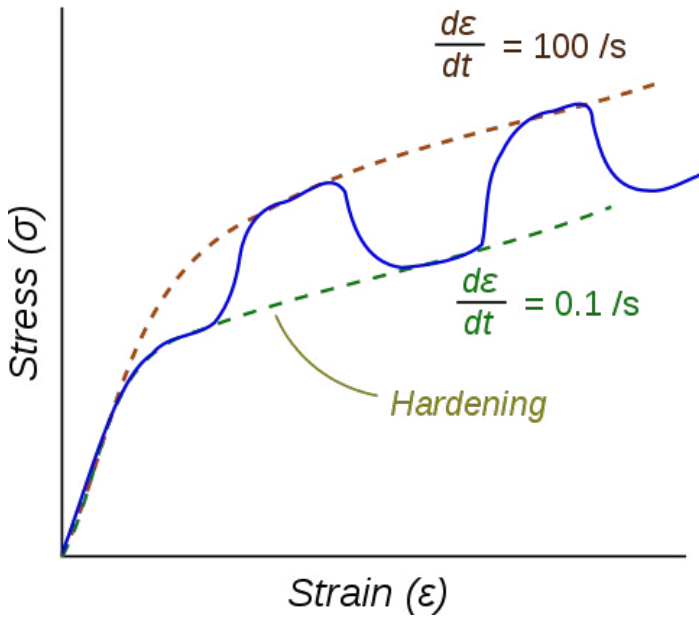


Figure 2: Stress-strain response of a viscoplastic material at different strain rates.

The dotted lines show the response if the strain rate is held constant. The blue line shows the response when the strain rate is changed suddenly.

One consequence of yielding is that as plastic deformation proceeds, an increase in stress is required to produce additional strain. This phenomenon is known as Strain/Work hardening. For a viscoplastic material, the hardening curves are not significantly different from those of rate-independent plastic material.

Nevertheless, three essential differences can be observed.

1. At the same strain, the higher the rate of strain the higher the stress
2. A change in the rate of strain during the test results in an immediate change in the stress-strain curve.
3. The concept of a plastic yield limit is no longer strictly applicable.

The hypothesis of partitioning the strains by decoupling the elastic and plastic parts is still applicable where the strains are small, i.e.,
 $\epsilon = \epsilon_e + \epsilon_{vp}$

where ϵ_e is the elastic strain and ϵ_{vp} is the viscoplastic strain. To obtain the stress-strain behavior shown in blue in the figure, the material is initially loaded at a strain rate of 0.1/s. The strain rate is then instantaneously raised to 100/s and held constant at that value for some time. At the end of that time period the strain rate is dropped instantaneously back to 0.1/s and the cycle is continued for increasing values of strain. There is clearly a lag between the strain-rate change and the stress response. This lag is modeled quite accurately by overstress models (such as the Perzyna model) but not by models of rate-independent plasticity that have a rate-dependent yield stress.”

Results

Figure 1 shows two stress-strain diagrams for DR risk versus lab A1C and finger A1C over two 6-year periods with a data comparison table.

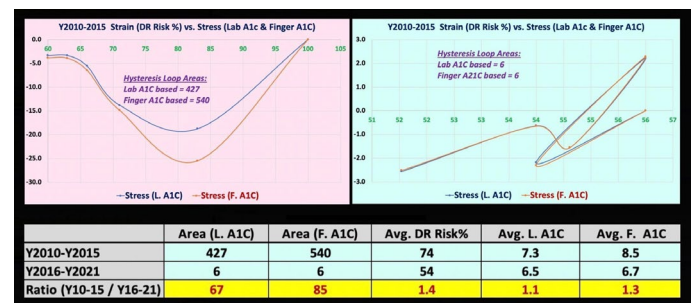


Figure 1: Two stress-strain diagrams for DR risk versus lab A1C and finger A1C over two 6-year periods with a data comparison table

Figure 2 displays the supporting data table.

4/8/22	Viscosity 1	Viscosity 2	DR Risk %	6	6		
DR vs. L.A1C & F.A1C	Lab-A1C	Finger-A1C	Strain (DR %)	Stress (L. A1C)	Stress (F. A1C)	Area (L. A1C)	Area (F. A1C)
Y2010	10.0	11.0	100	0.0	0.0	0	0
Y2011	6.6	9.0	83	-18.8	-25.5	160	217
Y2012	6.9	7.4	71	-13.8	-14.9	195	242
Y2013	6.7	7.8	66	-5.6	-6.5	49	53
Y2014	6.8	7.9	63	-3.4	-3.9	13	16
Y2015	6.8	7.7	60	-3.4	-3.8	10	12
Average or Sum	7.3	8.5	74	-7.5	-9.1	427	540
				Stress Ratio =	82%	Area Ratio =	79%
4/8/22	Viscosity 1	Viscosity 2	DR Risk %	6	6		
DR vs. L.A1C & F.A1C	Lab-A1C	Finger-A1C	Strain (DR %)	Stress (L. A1C)	Stress (F. A1C)	Area (L. A1C)	Area (F. A1C)
Y2016	6.6	7.0	56	0.0	0.0	0	0
Y2017	6.6	6.9	54	-2.2	-2.3	2	2
Y2018	6.7	6.9	56	2.2	2.3	0	0
Y2019	6.7	6.7	55	-1.6	-1.6	0	-1
Y2020	6.2	6.3	54	-0.6	-0.6	1	1
Y2021	6.3	6.1	52	-2.6	-2.5	4	4
Average or Sum	6.5	6.7	54	-0.8	-0.8	6	6
				Stress Ratio =	99%	Area Ratio =	100%
	Area (L. A1C)	Area (F. A1C)	Avg. DR Risk%	Avg. L. A1C	Avg. F. A1C		
Y2010-Y2015	427	540	74	7.3	8.5		
Y2016-Y2021	6	6	54	6.5	6.7		
Ratio (Y10-15 / Y16-21)	67	85	1.4	1.1	1.3		

Figure 2: Supporting data table

Figure 3 illustrates frequency energy analysis results.

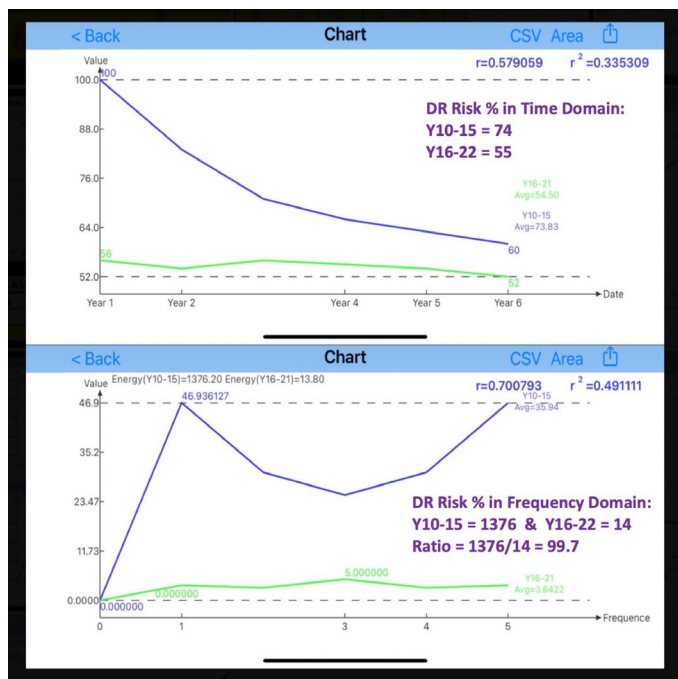


Figure 3: Frequency energy analysis results of DR risk %

Conclusion

In conclusion, the following five described biophysical characteristics have demonstrated the key behaviors of DR risk % using the approaches of both VGT energy and the frequency energy:

- (1) When his body weight drops continuously over these two 6-year periods, both the lab A1C and finger A1C values also decrease. His lab ACR and finger A1C have a strong correlation coefficient ($R = 86\%$). This reduction of lab A1C and finger A1C can be seen clearly from the attached data table. His 6-year average data of (lab A1C, finger A1C) are: Y10-15 = (7.3%, 8.5%) and Y16-21 = (6.5%, 6.7%). His 6-year average DR risks are: Y10-15 = 74% and Y16-21 = 54%.
- (2) Looking into the 2 average strain (DR risk %) values for the two periods, the Y10-15 period covers a DR risk range of 60%-100% with an average DR risk of 74%, while the Y16-21 period includes a DR risk range of 52%-56% with an average DR risk of 54%.
- (3) His annual lab A1C and finger A1C values within the two 6-year periods are continuously declining as time moves forward. This observed phenomenon provides a clue that the viscosity factors, $\eta = \text{lab A1C and finger A1C}$, are also decreasing as time moves forward. Therefore, the stress magnitudes based on lab A1C and finger A1C are reduced from the first 6-year period to the second 6-year period since stress is the strain rate multiplied by the viscosity factor of η . See the lab A1C stress-range, or lab A1C y-axis scale: Y10-15 = 19 (0 to -18.8) and Y16-21 = 5 (2.2 to -2.6). The finger A1C stress range for finger A1C y-axis scale is: Y10-15 = 26 (0.5 to -25.5) and Y16-21 = 5 (2.3 to -2.5). One observation is that the Y10-15 lab A1C stress ranges (-7.5) are fairly close to the Y10-15 finger ACR stress ranges (-9.1); while the Y16-21 lab A1C stress ranges (-0.8) are identical to the Y16-21 finger ACR stress-ranges (-0.8). It should be mentioned that the normalized factor for both lab A1C

and finger A1C is 6.0%.

- (4) The calculated 2 hysteresis loop areas are significantly reduced from the first 6-year period to the second 6-year period, the lab A1C area reduction rate is 67 while the finger A1C area reduction rate is 85. These two-loop areas represent the associated relative energy of DR risk under the influence of lab A1C and finger A1C within each period. See the lab A1C hysteresis loop areas: Y10-15 = 427 and Y16-21 = 6 and the finger A1C hysteresis loop areas: Y10-15 = 540 and Y16-21 = 6. Based on the above 4 loop areas, it is obvious that the VGT energies for the Y10-15 period are about 67 to 85 times higher than the Y16-21 period.
- (5) Using the frequency energy tool, the comparison between Y10-15 period versus Y16-21 are: average DR risk % in TD = 74% vs. 55% with a ratio of DR risk $5 = 74/55 = 1.35$, while the DR risk frequency energy in a FD = 1376 vs. 14 with a ratio of DR frequency energy = $1376/14 = 99.7$. This significant frequency energy difference of 99.7 is similar to the VGT energy difference of 67-85.

In summary, body weight influences glucose. The energy in glucose circulates with the blood flow inside the body. If we have excessive energy associated with hyperglycemia within the blood flow, it can damage internal organs to cause retinal complications, including DR.

From this study of biomarker data analysis within a long 12-year period which is grouped into two identical 6-year sub-periods, the energy ratios for the two periods (Y10-15 versus Y16-21) are re-listed in a simplified fashion:

- (1) Energy ratio of Y10-15 versus Y16-21 using VGT method: lab A1C loop area ratio = 67 to 1; finger A1C loop area ratio = 85 to 1.
- (2) Metabolism index-based CKD risk ratio of Y10-15 versus Y16-21 = 1.4 to 1.
- (3) Collected average lab A1C ratio of Y10-15 versus Y16-21 = 1.1 to 1.
- (4) collected average finger A1C ratio of Y10-15 versus Y16-21 = 1.3 to 1.

The two energy ratios of DR risk (both A1C-based and ACR-based) have similar patterns. When BW and daily glucose conditions improve, his DR risks are then reduced accordingly (by 40%); however, the associated energies with DR risks are decreased even more significantly (by 67-85 times if using the VGT energy method or 99.7 times if using the frequency energy method). It should be pointed out that his DR risk was remarkably reduced in the second 6-year period when his lab A1C and finger A1C dropped below 6.7% since the dividing year between healthy versus unhealthy in Y2016.

References

For editing purposes, the majority of the references in this paper, which are self-references, have been removed. Only references from other authors' published sources remain. The bibliography of the author's original self-references can be viewed at www.eclaircmd.com.

Readers may use this article as long as the work is properly cited, their use is educational and not for profit, and the author's original work is not altered.

Copyright: ©2022 Gerald C. Hsu. This is an open-access article distributed under the terms of the Creative Commons Attribution License, which permits unrestricted use, distribution, and reproduction in any medium, provided the original author and source are credited.